WILEY

Robot for weed species plant-specific management

Owen Bawden[1] (iD) | Jason Kulk[1] | Ray Russell[1] | Chris McCool[1] | Andrew English[1] |
Feras Dayoub[1] | Chris Lehnert[1] | Tristan Perez[1,2]

[1]Electrical Engineering and Computer Science, Queensland University of Technology, Brisbane 4000, Australia

[2]Institute for Future Environments, Queensland University of Technology, Brisbane 4000, Australia

Correspondence
Owen Bawden, Electrical Engineering and Computer Science, Queensland University of Technology, Brisbane 4000, Australia.
Email: o.bawden@qut.edu.au

Abstract

The rapid evolution of herbicide-resistant weed species has revitalized research in nonchemical methods for weed destruction. Robots with vision-based capabilities for online weed detection and classification are a key enabling factor for the specialized treatment of individual weed species. This paper describes the design, development, and testing of a modular robotic platform with a heterogeneous weeding array for agriculture. Starting from requirements derived from farmer insights, technical specifications are put forward. A design of a robotic platform is conducted based on the required technical specifications, and a prototype is manufactured and tested. The second part of the paper focuses on the weeding mechanism attached to the robotic platform. This includes aspects of vision for weed detection and classification, as well as the design of a weeding array that combines chemical and mechanical methods for weed destruction. Field trials of the weed detection and classification system show an accuracy of 92.3% across a range of weed species, while the heterogeneous weed management system is able to selectively apply a mechanical or chemical control method based on the species of weed. Together, the robotic platform and weeding array demonstrate the potential for robotic plant-species–specific weed management enabled by the vision-based online detection and classification algorithms.

1 | INTRODUCTION

Over the past century, agricultural productivity growth has been achieved through farm consolidation leading to greater economies of scale, increased mechanisation, crop improvements through accelerated breeding and genetic modification, as well as through the application of inputs including herbicide, fertilizer, and water. As countries have shifted to broadacre farming to increase food production,[1] crops and landscapes that were once tended by humans are now tended almost entirely using machines through large-scale mechanical and chemical interventions.

Increasingly larger vehicles combined with precision guidance systems have been designed and used to improve production on broadacre farms.[2] The benefits have been greater productivity, reduced labor cost per hectare, and an economical platform for the latest technological developments. However, this trend has resulted in new problems for farmers. As vehicle size has increased, so has the detrimental effect of soil compaction through the ground pressure of these vehicles,[3] while increased engineering complexity of the vehicle has resulted in disruptions due to single machine failures.

Within Australia, a high proportion of broadacre farmers now use zero-till agricultural practices to limit soil disturbance, resulting in reduced erosion, permanent ground cover leading to greater moisture retention, reduced input costs, and reduced soil compaction.[4] However, the nature of the practice requires greater use of herbicides to mitigate weeds, and this has led to increased herbicide resistance in weeds costing Australian agriculture around $4 billion dollars per year.[5] This has led to alternative approaches such as intercropping (growing two or more crops), alternate planting patterns, crop and cultivar selection, rotating crops, and tillage.[6–8] The field of agricultural robotics is responding to the challenges in the agricultural sector by developing robots that can operate with greater effectiveness, for longer hours and at less cost than traditional farm machinery and labor. Most importantly, robots can enable the use of alternative weed destruction—this is a consequence of robots operating at lower speeds and their ability to make decisions based on their perception. So far, robots have been slow in their translation to farming because of the unstructured environment of biological production processes and the inherent variability of biological systems.[9] In addition to this, the cost of mechanical technology, limited capacity, and potential legal risks are but a few of the challenges to be overcome.[10] Agricultural robots will be developed to work safely alongside humans across a broad range of environments to help improve agricultural efficiencies and boost crop yields,[11] with benefits including reduced crop

FIGURE 1 AgBotII during weed-management field trials in Dalby, QLD, Australia

wastage, pesticide usage, and energy consumption. Utilized as a system, coordinated fleets of robots may present solutions to the issues of soil compaction, single machine failure, and weed resistance, and offer the return to individualized plant care without the high labor cost.

This paper presents the development of an autonomous system for broadacre agriculture capable of undertaking a range of agricultural tasks, with a focus on weed management through mechanical intervention and precise spraying. The paper focuses on two key developments: the first is AgBotII, a lightweight and energy-efficient robotic vehicle with a configurable, modular design, enabling interchangeable implement units to span between the modular side units. The second is the plant-species–specific weeding array, a system that integrates vision-based plant detection and classification with targeted treatment of individual weed species. Plants are first detected by modeling their color distribution, then highly probable regions are classified by extracting visual texture-based features. Once a plant species has been classified, the best weed management method for a particular species can be deployed. This consists of a one-degree-of-freedom mechanical and precision spray array designed to target individual weeds. These two developments form part of a complete autonomous system for broadacre agriculture and extend the work presented in Ref. 12, significantly expanding on the full platform and the weeding array development. Figure 1 shows the AgBotII during field trials undertaking weed management.

Results from the field trials demonstrate that the robot can successfully perceive and classify in-field, achieving an accuracy in excess of 90% across a range of weed species. The weeding array was used in-field to selectively apply, based on the weed species, mechanical weed removal or a precise herbicide application.

The rest of this paper is organized as follows. In Section 2, we review the state of the art in robotic platform development and autonomous nonchemical weed management. Section 3 covers our stakeholder engagement and insights, and outlines the functional requirements and specifications for the platform and implement design. Sections 4 and 5 detail the robot and weeding array design, respectively. Section 6 contains the results from experiments and field trials, and we then conclude with a discussion of the results and lessons learned.

2 | STATE OF THE ART

This section reviews the state of the art in robotic platform development for agriculture.

2.1 | Robotic platform development for agriculture

Vehicle design has been researched and developed extensively since 1886 with the design of the first automobile by Karl Benz. The work of Bekker[13,14] and Wong[15] on vehicle mobility, off-road locomotion, and terramechanics, and the work of Apostolopoulos[16] on the analytical configuration of wheeled robotic vehicles, has been well-referenced in the design of specialist vehicles. The work of Madsen and Jakobsen,[17] Åstrand and Baerveldt,[18] Jensen et al.,[19] and Bakker et al.,[20] among others, has described the design of autonomous platforms, predominantly for experimental robotic weeding. Their design approach has varied due to considerations of traction, steering, dimensions, power-supply, and control architecture. Madsen and Jakobsen[17] developed an experimental four-wheel-drive (4WD), four-wheel-steer (4WS) platform for the purpose of testing software, navigation, and different steering approaches. This battery-powered vehicle could operate for 2–4 h, and it was designed for driving in-crop with 500 mm of ground clearance and a narrow wheel-transmission setup. Along similar lines, but developed for the task of weed control in sugar beet fields (a crop grown widely in Europe for sugar production), Åstrand and Baerveldt[18] designed a mobile robot as an experimental platform with a two-wheel-drive (2WD), two-wheel-steering (2WS) Ackermann configuration. This robot was battery-powered for indoor use, and a petrol generator was used for field trails. It utilized a mechanical weeding tool consisting of a spinning wheel rotated perpendicular to the crop row to manage weeds in the inter-row area.

More sophisticated configuration adjustment was incorporated into the BoniRob,[21] developed primarily for plant phenotyping experiments. This robot has recently been licenced by Bosch-startup Deepfield Robotics and is being developed for commercialization as an agricultural robotics platform. The design incorporates individual wheel drives, adjustable ground clearance (40–80 cm), and track widths (75–200 cm). The vehicle can be powered by either batteries or a petrol generator for field trials.

The majority of robotic agricultural platforms designed until now have been four-wheeled vehicles with either two- or four-wheel steering. These include the Hortibot,[22] Weedy Robot,[23] Zeus,[24] and Ladybird.[25] Developments in autonomous tracked vehicles have also occurred, such as the Spirit Tractor[26] and Armadillo.[19] The Armadillo was designed as a mobile implement carrier, incorporating track modules mounted on the side of an exchangeable implement. This system allows for height and width adjustment of the platform. Brixius and Zoz[27] and Molin and Leviticus[28] outlined the performance characteristics of tracks, including improved traction, higher pull ratios, and reduced soil compaction, while the drawbacks are increased mechanical weight, complexity, cost, and soil disturbance through skid steering. In the case of the Armadillo, each track module includes a motor controller, an electric motor, and a transmission, and it is controlled by a computer integrated into the implement section of the vehicle. In 2013,

a modified version of the Armadillo named the Vibro Crop Robotti[29] was commercialized by Kongskilde Industries and Conpleks Innovation.

Determining the power requirements for the platform is an important consideration of the design process. A vehicle carrying an implement for soil cultivation tasks, such as mechanical hoeing, will require more power than a robot selectively spraying herbicide. In the case of the Armadillo,[19] power for the track modules is supplied by the implement as well. This allows the use of various power sources such as battery packs or an electrical generator, depending upon the requirements of the implement. The Mobile Robot[18] and the Bonirob[21] utilized batteries for indoor testing and swapped to an internal combustion driven generator for field tests.

The work of Day[9] highlights the fact that ongoing research and development into robotic platforms for agriculture has led to the integration of technology from other industrial sectors, including automobile and aerospace manufacturing, where research has gone into developing platforms incorporating stronger and lighter materials. This is assisting the manufacture of lightweight agricultural vehicles and helping to achieve the key goal of reduced soil compaction.

2.2 | Computer-guided Weed Management

Two examples of commercial systems that perform intrarow cultivation with computer-vision systems are the Garford Robocrop InRow Weeder[30] and the Steketee IC automatic hoeing machine.[31] These commercial tools have been used for crops such as lettuce, cabbage, onion, sugar beat, maize, soy beans, flowers, and cereals. The Robocrop integrates a disc hoe with a specialized cutout and a computer-vision system to perform precise intrarow cultivation.[30,32] As the cultivator moves down the crop row, the orientation of the disc's cutout is in phase with the position of the crop in order for the swept cultivated area to pass between the crop. The Robocrop system is reported to achieve a top speed of three crops per second (5 km h^{-1} for an inter-row spacing of 0.25 m).

A guided cycloid hoe has been previously designed for inter- and intrarow cultivation, primarily for maize crops.[33,34] The cycloid hoe consists of a vertical rotor with eight tines attached in a circle. As the tractor travels in a linear direction, the tool rotates causing the tines to cultivate a cycloid path while avoiding damage to the crop. A real-time kinematic (RTK) global positioning system (GPS) is combined with a prior seed map of the crops positions to determine actuation of each tine. However, the disadvantages of using RTK-GPS for crop seed mapping is that it relies on having a good GPS signal.

Computer-guided hoes have been used for inter-row weed control[35] and they have been developed commercially.[36,37] These devices use a hoe blade that can retract to avoid crops. When a crop is detected via a computer-vision system, the blades are folded inward to avoid disturbance to the root zone of the crop. Results from field trials show that the guided systems can work up to speeds of 4 km h^{-1} with little damage to crop roots at a crop spacing of 300 mm. At 8 km h^{-1}, 17% of the crop root zone was affected[35] and approximately 83% of weeds were successfully controlled at a speed of 3 km h^{-1}.[38]

2.3 | Robotic weed control

Robotic weed control has been implemented using electrodes fitted on the end of a delta arm parallel kinematic manipulator.[39] The platform has been tested for weed control within a lettuce crop and was pulled by a conventional tractor. The disadvantage with using electrodes is that a large amount of energy is required per weed, making it less suited for a mobile robot. A spot weed destruction tool called the tube-stamp uses a mechanical stamp surrounded by a tube to destroy a weed by pushing it into the soil.[40,41] The tube-stamp has been mounted successfully to the BoniRob robot platform. The effectiveness of the tube-stamp was evaluated experimentally in a greenhouse and in-field for different weed species, and the results indicated that the mechanism may not work for all types of weed species, such as grass weeds.[40]

The Ladybird[25] is equipped with a six-axis robotic manipulator for weed destruction, and it has the capability of conducting autonomous farm sensing and manipulation tasks for various vegetable crop varieties. The RIPPA^{TM} incorporates either a precision spray system or a single two-degrees-of-freedom mechanical implement.[42]

An agricultural robot developed by ecoRobotix[43] is a vehicle for inter- and intrarow weeding that utilizes a slender chassis and delta-arm with a liquid-spray or rotating-blade end effector. Another agriculture robot featuring a spinning blade was described by Van Evert[44] and it is aimed at killing a specific broad-leaved dock weed. The effectiveness of this spinning blade mechanism was shown to be between 60% and 80%.[45]

Research into applying chemical directly to weeds using a robot arm was reported by Jeon and Tian.[46] The robot tool incorporates a small cutting tool that makes a cut on the weed, exposing the plant's vascular tissue, and a micropump to apply chemical to the surface of the cut. Although the technique reduces the amount of herbicide used, the main disadvantage involves the time and the precision required to make incisions in each weed.

2.4 | Detection and classification

Weed detection is undertaken using either common (RGB) cameras or camera systems utilizing both near-infrared (NIR) and color information. The use of color cameras for the detection processing is common due to their low cost and availability; however, detection using NIR information takes advantage of the way that plant leaves greatly reflect NIR light.[47]

The common approach to performing weed detection using both RGB and NIR is based on vegetation index images.[48] Vegetation indices using RGB images include the excessive green (ExG) and normalized excessive green (NExG) indices, color index of vegetative extraction (CIVE), vegetative (VEG) index, and excessive green minus excessive red (ExG-ExR) index. These have been used in multiple works to perform plant-dirt segmentation, such as in Refs. 49–51. In comparing some of these different vegetative indices, however, Meyer and Neto[52] found that ExG-ExR gave an improved segmentation accuracy by reducing the number of false positives generated when using ExG or CIVE. When including NIR information, the most commonly used vegetative index is the normalized difference vegetation index (NDVI),

which uses a ratio between the amount of NIR light and red light reflected by objects.[53]

More robust color spaces than RGB have been investigated in the literature. Suh et al.[54] converted RGB images to an illumination-invariant xyY color space to perform their segmentation. Another work that investigated using different color spaces was performed by Ruiz-Ruiz et al.[55] This method used the hue and saturation components of the HSV color space to perform an environmental adaptive segmentation algorithm (EASA). The EASA was developed for segmenting plants and dirt while being adaptable to environmental changes such as illumination changes. An analysis of several different color spaces for plant segmentation was performed by Philipp and Rath.[56] The Lab, Luv, and HSV color spaces were found to be effective for detection. Finally, machine-learning methods have also been developed for performing plant segmentation. A machine-learning approach to plant segmentation was used[57] to achieve qualitatively superior segmentation results to those of ExG and NDVI.

Using the above techniques for green/dirt segmentation, a variety of visual characteristics of weeds have been used in order to identify weed species. The most common visual characteristics (i.e., features) are shape and texture.

Shape features can be created after segmentation from the morphological properties of weed leaves.[58] The most common shape features used in the literature are aspect ratio, roundness, circularity, convexity, and ratios among length, width, perimeter dimensions, elongation, central moment, and principal axis moment shape. Recent works using these features can be found in Refs. 49 and 59. The main problem with shape-based features is the fact that in realistic farm conditions, the weeds can be overlapping or occluded. This means that complete leaf edge information or leaf orientation can be missing, which impacts the performance of the classification system. To overcome this shortcoming in shape-based features, texture features have been used within the literature.

Two commonly used texture features are the local binary pattern[60] (LBP) features and covariance features (Cov.).[61] Both have a rich history in computer vision as they are computationally efficient and have been shown to be effective for a range of object-recognition problems. The LBP feature has been used for object recognition tasks including texture classification,[60] face recognition,[62] and crop detection.[63] It is computationally efficient and robust to illumination variations as it is computed by performing a set of pixel comparisons. Covariance features have been used for general object recognition,[61] material classification,[64] and action recognition.[65] They capture the gradient information from an area and then represent this compactly using a covariance matrix.

3 | SYSTEM REQUIREMENTS

The development of a mobile robot for agriculture represents a significant investment in terms of time and cost. When undertaking the research, design, engineering, prototyping, testing, and iterations necessary to put a robot in the field, it is often the quality of early insights—the understanding of "why" from stakeholders—that is most critical.[66] These insights are used to establish the functional requirements that must balance the complex demands of the system and the needs of the user operating in an unstructured environment. The incorporation of a user-centered design methodology[66] helped uncover key insights during the development of the AgBotII.

3.1 | A farmer's perspective

Redhead et al.[67] asked farmers and agronomists to participate in contextual interviews and observational studies at farm locations in the Darling Downs and Emerald regions in Queensland, Australia (see Fig. 2). The purpose of the field studies was to develop a better understanding of current farming practices, hear the farmers' thoughts about incorporating agricultural robots in their farming practice, and to further appreciate the farmers' perspective on task automation, in order to inform design decisions that address both technology-specific features and usability issues. The relevant insights from the study are provided below; for complete results, the reader is referred to Ref. 67.

The farmers interviewed highlighted the importance of good weed control in their operations and the consequences, in subsequent years, of allowing weeds to seed. A major challenge identified by the farmers is herbicide resistance and the associated costs of applying increased dosages, or using specialized and expensive chemicals to control weeds. Blanket spraying is the primary means of controlling weeds during fallow periods. Surviving herbicide-resistant weeds are either individually "spot"-sprayed using higher concentrations or alternative chemical compositions, or removed by hand. Removing individual weeds by hand is referred to as "chipping out," which involves using a hoe or similar kind of bladed tool. Farmers described chipping out as a difficult, labor-intensive, and time-consuming task; however, this method is common practice for efficient and economical weed control. Spot spraying can be done manually or with technology such as a WeedSeeker® attached to a tractor. However, these rigs are expensive and some farmers described the difficulty of achieving sensor accuracy across wide 36–48 m spray booms. The farmers interviewed envisage agricultural robots as being most useful in taking over the roll of chipping out weeds, as this would enable a decreased expenditure on herbicide, and it would free up labor currently dedicated to hand hoeing.

Farmers noted that the reliability of autonomy is a big issue with unstructured farm conditions, including varying crops and crop heights; wheel tracks that are washed out, wet, boggy, or cracked; and undulations in the land. Farmers were cautious about the endurance of robots and the level of monitoring and attention that may be required in a broadacre farming environment. However, part of their work involves thinking through mechanical design problems, and overall they were enthusiastic about the potential of autonomous platforms and were keen to test prototypes. Additionally, the farmers were interested in the idea of assembling their own robots from "flat-packed" kits for early prototype testing on their farms. While this is a business/economics research solution for prototype production, the farmers welcomed the opportunity for hands-on involvement in prototype development, to give feedback for follow-on iterations, and

(a) Field studies undertaken on broadacre farms.   (b) Review of currently used farm machinery.

FIGURE 2 Contextual interviews and observational studies were undertaken at farm locations in the Darling Downs regions (west of Toowoomba) and around Emerald in central Queensland, Australia

they acknowledged the potential of flat-packed kit robots as a feasible solution for future investment.

3.2 | Design implications

The following list consolidates the insights from field studies, conducted in Ref. 67, and the implications on the design and development of agricultural robots (AgBots):

- AgBots are most suited to precision work that requires accuracy, which is difficult to achieve across large machinery, such as 48 m boom sprayers.
- Farmers are competent at, and interested in, thinking through mechanical build problems, and participatory engagement of farmers in the design, testing, and iteration of AgBot prototypes would be beneficial to the farming community and ongoing research.
- The mechanical build of the system should remain open for ongoing maintenance and adaptability.
- Varying levels of access to the interface system are necessary, with a simple level of control available for nonskilled labor, and more complex levels of administration by farm managers or consultants.
- Rural communication infrastructure cannot be assumed to be adequate for reliable remote access, and should be addressed as part of the design of robots.
- Farmers welcome an open-source community model for the software development of AgBots, and this should be set up early and in a way that encourages participation from farmers.
- The ratio of operators to AgBots needs to be manageable in terms of the workload for monitoring and maintaining these vehicles.
- Remote views of AgBots should give adequate and easily interpreted visual information about the state of the machine and the nature of failure modes.

The user research and the insights gained from field studies with farmers were used to establish a detailed list of Functional and Operational Requirements for the development of the AgBotII, and it is presented in Ref. 68.

TABLE I AgBotII main technical specifications

	Specification	Magnitude (target)	Unit
TS_1	Vehicle mass	500	kg
TS_2	Payload mass	200	kg
TS_3	Operational speed	5	km/h
TS_4	Maximum speed	10	km/h
TS_5	Number of wheels	4	–
TS_6	Drive wheels	2	–
TS_7	Steering wheels	2	–
TS_8	Wheel width	0.3	m
TS_9	Width (wheel center to wheel center)	3	m
TS_{10}	Length total	2.5	m
TS_{11}	Implement section clearance	0.75	m
TS_{12}	Operating gradient pitch	15	%
TS_{13}	Operating gradient roll	10	%
TS_{14}	Handle emergency brake	–	–

3.3 | Technical specifications

Based on the functional and operational requirements and input, we conducted a detailed tradeoff study and determined the main *technical specifications* shown in Table I.

Vehicle mass (without payload) (TS_1): Consulted farmers suggested that all-terrain vehicles (ATVs) used for farming resulted in minimal soil disturbance when driven over fields in varying conditions. ATVs range in size and mass from 200 to 600 kg; therefore, based on this and the required strength, we estimate the target mass to be 500 kg for the vehicle.

Payload mass (TS_2): To dimension the mass of the payload, we considered weed management with current spot-spraying technology. Based on a 3 m width, an operational speed of 5 km h^{-1}, and a spray rate of 15 L ha^{-1}, a 200 L tank would require refilling every 10 h. Given the inclusion of the mechanical weeding array, we expect to use less than 15 L ha^{-1}; however, the payload must also account for the development of future implements, so a target weight for the payload of 200 kg was adopted.

Operational speed (TS_3): The target operational speed of 5 km h^{-1} was selected according to safety, coverage based on an operational
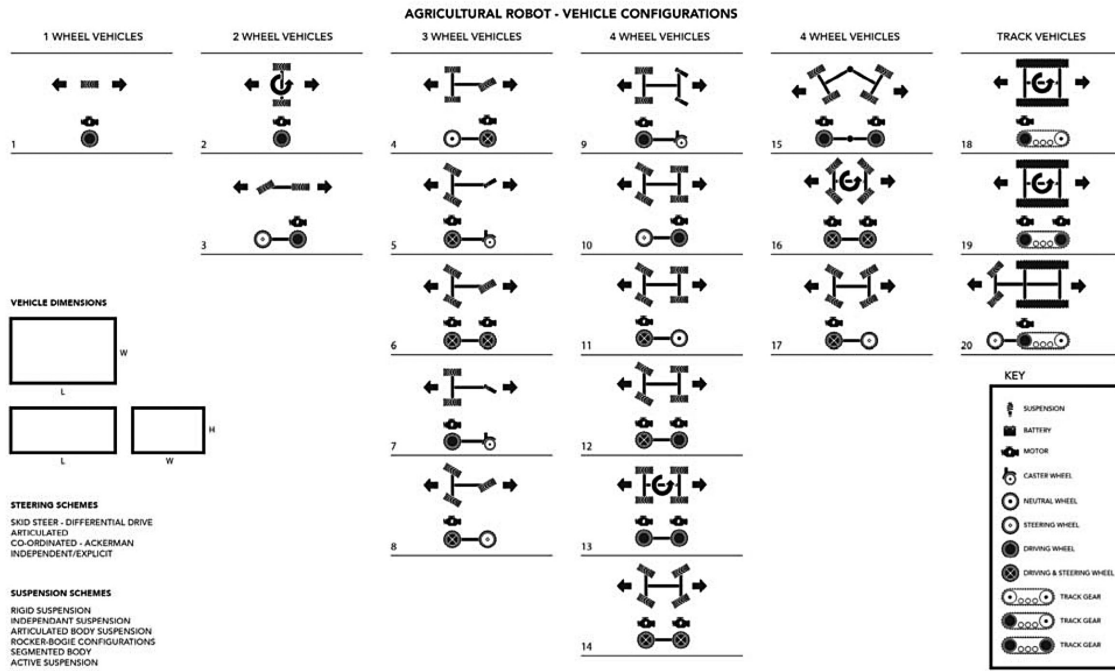
FIGURE 3 Twenty vehicle configurations, including both tracked and wheeled variants, were analyzed in relation to the above considerations

cost model, and timing requirements for the computer vision system to process data for weed detection and classification. The average walking speed of a human is 5 km h^{-1}, so humans could easily overtake the robots.

Maximum speed (TS_4): The maximum speed is selected for traveling to recharging/replenishment stations and to move from paddock to paddock. Given the operational speed, the maximum target speed has been determined based on potential use of gearboxes and hydraulic drive trains and the range of speeds of electrical motors, which are to be optimized for maximum efficiency at the selected operational speed.

Vehicle configuration (TS_{5-7}): Analysis of vehicle configurations, shown in Figure 3, took into account considerations of manoeuvrability, stability, locomotion type (tracks vs wheels), the number of drive and steering motors, and motion control design. A four-wheel configuration, capable of bidirectional driving through the use of differential steering and caster wheels (configuration 9 in Figure 3), was selected as the configuration for further development. This configuration offers an appropriate balance between driving performance, stability, payload capacity, and complexity.

Vehicle dimensions (TS_{8-11}): A standard row width of 0.5 m would be appropriate for a large portion of broadacre applications. With allowance for overhanging leaves and drift in steering, a working width of 300 mm was considered safe for the wheel unit. To move the AgBotII on Australian roads[69] requires that the width of a vehicle must not be over 2.5 m. Hence, to move the AgBotII on a typical flatbed trailer, the length (or width, depending upon the orientation of the AgBotII to the truck/trailer) needs to be less than 2.5 m. Based on current control traffic farming (CTF) practices, a vehicle width (wheel center to center) of 3 m was chosen. This enables the AgBotII to take advantage of the CTF layout already in place on many broadacre farms. Being wider than the

width permissible for carriage on a public road means that the vehicle would need to be loaded perpendicular to the truck or trailer used for carrying the AgBotII. Broadacre crop heights vary according to region, crop variety, moisture availability, soil nutrients, and weed competition. Based on average crop heights of wheat, barley, sorghum, oats, cotton, and chickpea, we determine that the vehicle clearance should be at least 0.75 m, with the option for small adjustments based on suspension settings.

Operation (TS_{12-14}): Broadacre farming is generally undertaken on relatively flat terrain. Operating gradients of 0–3% are very common. Paddocks with 5–10% gradients are less common because the land is more energy-intensive to cultivate. Based on farm research, an operating gradient of 15% was estimated as the worst case that the agricultural robot would encounter in field conditions. In terms of side constrain forces of wheels, a 10% gradient is considered to be the worst case for roll angle operation. It is also a technical requirement that the vehicle must not tip over during emergency braking in gradients of ±15%.

3.4 | System overview

The complete robotic-agricultural system consists of the farmer, his robot with the weeding implement, and the robot's garage, as illustrated by Figure 4. The farmer interacts with the AgBotII via a virtual globe software interface for autonomous control and a radiofrequency remote for manual control, as required.

The AgBotII is a small, lightweight robot platform for broadacre agriculture. The robot has been designed to be modular, available as a ready-to-assemble kit, and to have a large, flat, multipurpose area for the attachment of weeding implements. The AgBotII has a single downward-facing camera with a lighting module for weed detection

FIGURE 4 The AgBotII with weeding implement attached, docking with the solar-powered recharge station

FIGURE 5 AgBotII platform rendering showing the major assemblies

and classification. The AgBotII is entirely self-contained with all processing done onboard. The key features of the AgBotII platform are described in Section 4.

The weeding payload for the AgBotII described in this paper consists of a heterogeneous weeding array, capable of treating weeds with either herbicide or a mechanical tool. The weeding array is described in detail in Section 5.

4 | ROBOT-VEHICLE DESIGN

The mechanical design of the robot is comprised of seven major vehicle assemblies: the modular side units, implement unit, battery boxes, swing arms, drive units, caster assemblies, and external covers. Figure 5 depicts the relationships of these major assemblies to one another with respect to the overall vehicle design. Due to the symmetrical construction of the vehicle, four of the seven assemblies are mirrored and occur on both sides of the vehicle.

A key operational feature of the robot is its flexibility to be reconfigured for multiple operations. This is achieved by its modular design with the two symmetric side units and the connecting implement unit, which can be adapted to carry different types of implements. The implement unit can also be adapted in width so as to match specific crop-row layouts. Although it is beyond the scope of the AgBotII prototype, the height of the robot could also be easily modified in order to accommodate crops of varying heights.

Novel design aspects of some of the major component assemblies, including the drive units, chassis design approach, implement hardpoints, and electrical system, are described in the following section. For a detailed discussion of the overall mechanical and electrical design of the robot, see Ref. 68 .

4.1 | Chassis design

Based upon our interactions with farmers, a novel construction method was developed that takes advantage of the considerable manufacturing infrastructure that already exists on most large farms in Australia. Due partially to their remote geographical location, most are mechanically self-sufficient, with nearly all farmers having the ability to
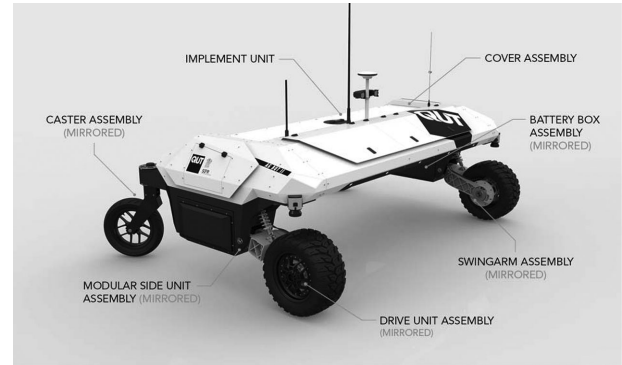
fabricate, repair, and maintain their own vehicles. By eliminating both the labor and facilities needed for producing complete vehicles, initial kits could be offered to farmers at a price substantially lower than a traditional, fully assembled robot would typically cost—especially given the initial low production volumes expected. This could deliver a large number of units into the hands of farmers without the need for significant infrastructure buildup normally required for vehicles of this size.

Using information gathered from our farm interviews and tours, we formulated a design strategy incorporating CNC laser cutting, pressing, and machining to rapidly produce, at low volumes and low cost, complete prototypes or kits that could be shipped to farms and assembled on-site by the farmers themselves. Using nothing more than a MIG welder, pneumatic rivet gun, and simple hand tools, the mechanical portion of the robot chassis itself can be assembled by two people in less than 8 h. An added benefit of this farmer-built strategy is the creation of an engaged community of users, always critical when developing a product that has the potential to challenge the status quo.

The modular side units function as the chassis for carrying the battery boxes, caster wheels, swing arms, and implement unit. Figure 6(a) shows the side-unit assembly. A unibody structural approach was taken to support the vehicle loads via the external skin of the chassis. Using a tab and slot concept, we have been able to create a jigless design that requires no specialized fixturing to manufacture. MIG welds are used to secure the panels together. This style of manufacturing and assembly removes the issues of alignment of the skin to the bulkheads, a time-consuming assembly procedure that requires a separate welding jig structure to be designed and built.

The unit is fabricated from a mild steel sheet that has been CNC laser cut and folded. Mild steel was selected as the material choice for the initial prototype because of the ability to quickly modify the chassis via welding if issues were discovered during testing.

Laser cutting sheet materials directly from two-dimensional (2D) CAD files minimizes part setup and tool changes common in other fabrication methods. Repositioning components for subsequent machining increases production time and may lower accuracy relative to machining operations made in one take. Laser cutting is also a relatively inexpensive material processing technology compared to hand fabrication or CNC machining. An additional characteristic of this design
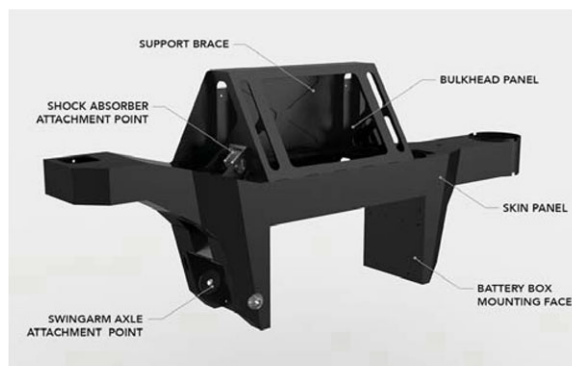
(a) Detail of the side unit assembly for the AgBotII.

(b) Flat-pack components for the side unit prior to assembly by MIG welding.

FIGURE 6 The side unit assembly for the AgBotII incorporates a tab and slot construction method and unibody structural approach in its design

is that all metal pieces can be cut and flat-packed, as indicated in Figure 6(b).

The implement unit, as seen in Figure 7(a), spans between the two side units. Its function is to set the width of the vehicle, stabilize the side units to prevent misalignment when driving, and to carry a payload of sensors, electronics, implements, and liquids for various agricultural and experimental tasks. The unit is constructed from CNC laser cut and folded components, and it is fabricated entirely from three specific grades of aluminum: 5005, 5083, and 6060-T5. The design incorporates a semi-monocoque construction with a stressed skin bracing five longitudinal cross spans and interlocking bulkhead components. The design is typical of aerospace structures for which light weight and high strength are required. Rivets are used to secure the cross span, bulkhead, and skin panels together. Several panels have been designed to be removable for access to internal equipment.

A requirement for the implement unit was the ability to carry various tools, such as the weeding array, for agricultural tasks and experimentation. To achieve this, a method of bolting components to the implement was included in the form of stainless steel "hardpoints" mounted to the inside of the five cross rails [see Fig. 7(b)]. The hardpoints are machined from 304 stainless steel for high strength, given the uncertainty we have as to what tools and features will ultimately be attached to the implement structure.

4.2 | Drive and power systems

The main drive units for the AgBotII consist of a customised motor, gearbox, and emergency brake assembly mounted inside a 14-wheel hub. When significant research failed to identify a suitable commercially available complete drive unit, a custom solution was chosen. Consideration of the vehicle's drive and power requirements, in conjunction with the torque, efficiency, and load specification of the individual components, allowed us to build an assembly capable of meeting the vehicle's operational specification.

A 5 kW, 48VDC electric motor, with an efficiency of 75–85% at 3200–4500 rpm, was paired with a 61:1 two-stage planetary gearbox to provide energy-efficient locomotion at the desired speed range of 5–10 km h^{-1}. Customized mounting plates mate the motor and gearbox to reduce the overall width of the assembly. The motor's output shaft was redesigned to allow for the addition of a fail-safe electric brake, which is mounted directly to the rear face of the motor via a modified friction plate. The fully assembled drive unit is depicted in Figure 8. The entire drive unit assembly is mounted to the vehicle's single-sided swing arm via a support cage, which transfers the load from the gearbox mounting flange to the swing arm. The custom wheel center, machined from billet aluminum, is mounted directly to the gearbox output flange.

The AgBotII has two battery boxes mounted centrally to the modular side units. The mounting position helps keep the vehicle's overall center of mass low so that the robot will not tip over during emergency braking.[12] However, placing the batteries in this position significantly restricted the available space to 300 mm to allow for in-crop driving. This restriction necessitated a custom solution to maximize the available capacity. The boxes were made using the same construction method as the implement unit.

Each battery box houses 16–100 Ah lithium iron phosphate cells, loaded into four subpacks of four cells each. Along with the cells, each battery box has a separate internal shelf that contains the battery management system. The internal subpacks make the assembly of the heavy packs more manageable and allow for the replacement of cells as they fail. Both of the battery boxes are self-contained. Each box is capable of powering the entire robot, providing a level of redundancy in the case of a pack failure. The battery box is shown in Figure 9.

The core component of the battery management system consists of a Tritium IQ.[70] There is a large contactor on both positive and negative terminals to provide redundant battery isolation, a current shunt, a small backup battery, and a microcontroller to implement custom battery management functions to improve integration and charging.

4.3 | Electrical and software systems

The main electrical components of AgBotII are shown in Figure 10. The two battery packs described in Section 4.2 are connected in parallel to form a 48 V battery with a capacity of 10.5 kWh, providing the AgBotII
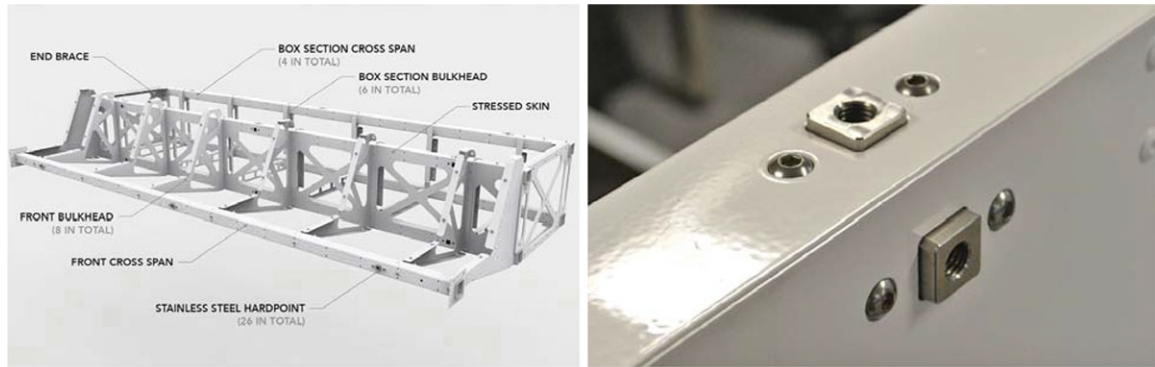
(a) The implement unit showing internal structural details.

(b) Structural hardpoints embedded in the implement unit are used for attaching tools used for agricultural tasks.

FIGURE 7   The implement unit is designed with a semi-monocoque construction from CNC laser cut and folded components, riveted together
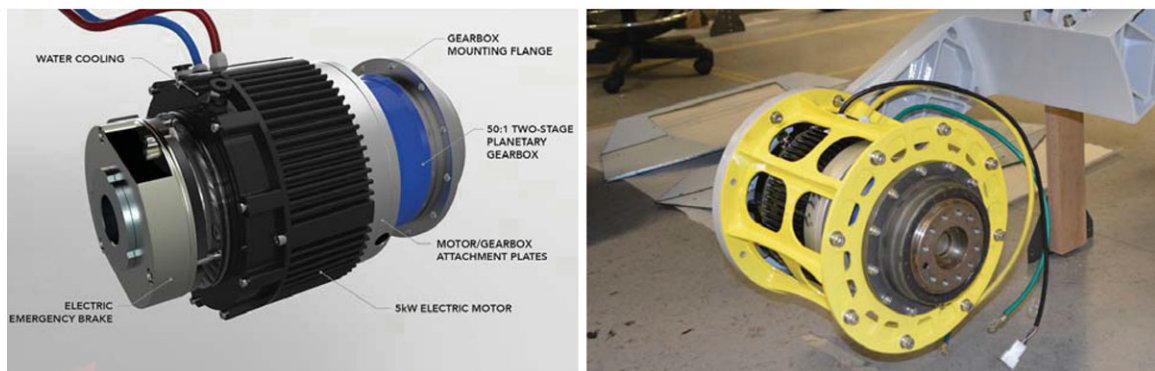
(a) Detail of the drive unit assembly for the AgBotII.

(b) Drive unit attached to the the single-sided swingarm

FIGURE 8   The custom gearbox-motor-brake drive unit assembly for the AgBotII
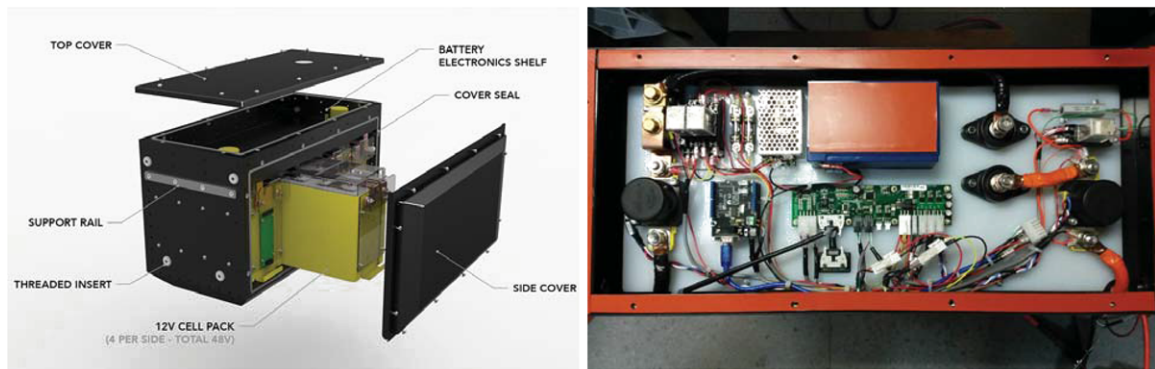
(a) Detail of the battery box assembly for the AgBotII

(b) Battery management and supporting electronics

FIGURE 9   The left battery pack designed and installed on the AgBotII

with between seven and eleven hours of autonomy. The motor controllers on the AgBotII are Roboteq MBL1660. An interesting feature of these motor controllers is that they can run custom firmware scripts. This allowed a very tight integration between the motor controllers, the safety system, and the navigation computer.

AgBotII uses a custom safety system designed to provide a simple user interface to the platform while providing a very high level of safety. The main components are a Hetronic NOVA-L wireless remote control and a Phoenix Contact PLC. The remote is used to control the safety state machine and to drive the AgBotII in manual mode. The safety system has also been designed to have a level of redundancy such that the emergency stop will continue to work if there is a single failure. Furthermore, that failure will be detected, and reenabling will be prevented until the failure has been fixed. This was implemented on the PLC and includes additional signal wires to check for contact welding on motor and payload contactors.
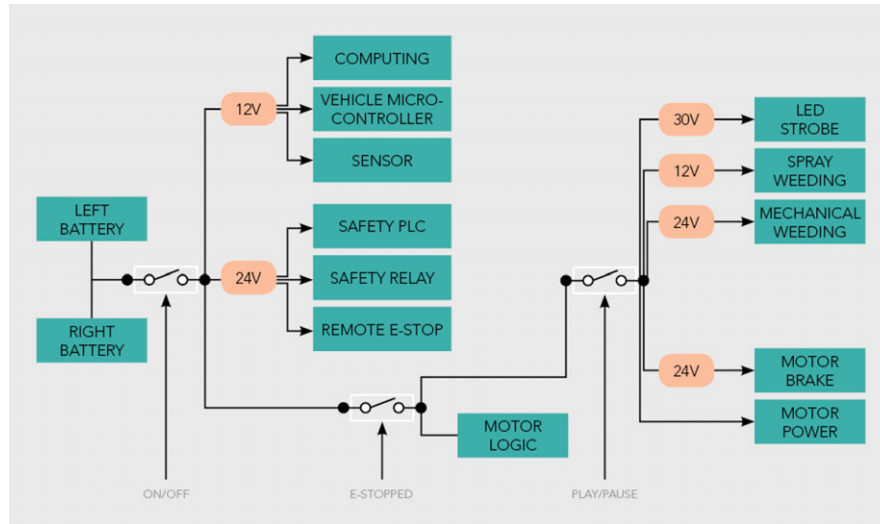
FIGURE 10 Overview of the safety and electrical systems on AgBotII

AgBotII has two quad-core Intel i7 computers, one used for navigation and the other for perception. The perception computer has a Nvidia GTX960 graphics card for parallel processing. The AgBotII also houses three microcontrollers in various locations to provide digital outputs for interacting with the safety system, weeding payload, and battery.

The software for the AgBotII is built upon the robot operating system (ROS) framework and split across two computers. The navigation and core functions are run on the first computer, as shown in Figure 11. The perception software is run on the second, more powerful, computer, which is detailed in Section 5.

The navigation has three main stages: coverage planning, guidance, and rate control. The coverage planner accepts a description of the field, obstacles, and row spacing to produce a sequence of waypoints that traverses every row. The path is created by sweeping lines parallel to the crop through the field.[71] When there are multiple rows that could be traversed next, such as those introduced by obstacles or concavity in the field, the path with the minimum total distance is selected by a brute-force search. The ordered waypoints are then given to the guidance module that uses a Novatel SPAN-IGM-A1 with RTK corrections for localization. To minimize the error between the robot's location and the target crop row, a PD controller on the heading to the line formed by consecutive waypoints is used. The module uses simple trapezoidal velocity curves based on the distance from the waypoint for speed control. Finally, the rate controller uses two proportional-integral-derivative (PID) controllers, one for each wheel, to track the target wheel speeds. Velocity feedback is provided by the inertial measurement unit (IMU) at a rate of 50 Hz and the motor pulse-width modulation (PWM) is controlled.

5 | PLANT-SPECIES–SPECIFIC TREATMENT SYSTEM

The plant-species–specific treatment system for the AgBotII incorporates a vision system, a selective mechanical weeding system, and a selective spray system. Individual weed species can be targeted by either the mechanical or spray system, depending on the result of a vision-based weed detection and classification system. An overview of the weeding system attached to the AgBotII can be seen in Figure 12. For the purposes of the first prototype, the module was designed to have a width of 1 m; this can be extended to the full width of the robot in future iterations.

The treatment of a weed occurs over the three stages shown in Figure 13. First, the weed is detected using a ground-facing camera and an image-processing computer. The image of the weed is then used by the weed classification to determine the species of the weed. Finally, the system selects the appropriate weeding implement and activates the weeding tool at the correct time as it passes underneath.

5.1 | Weeding actuation type selection

The implement designs considered during the design process can be broadly grouped according to the number of degrees of freedom required to actuate each weeding implement:

- 1 Degree-Of-Freedom (1DOF): An array of identical weeding implements arranged side by side or staggered. Each weeding tool may be actuated individually to engage the ground. This configuration may treat multiple weeds simultaneously.
- 2 Degrees-Of-Freedom (2DOF): A single weeding implement that slides sideways to align with oncoming weeds and actuated downward to remove each weed. This configuration can only remove one weed at a time, and weeds that are side-by-side may be missed.

In this section, we provide a theoretical analysis of the weeding capacity of both weeding mechanism actuation types in order to assist in making design decisions for the mechanical weeding implement.

5.1.1 | 1DOF weeding mechanism analysis

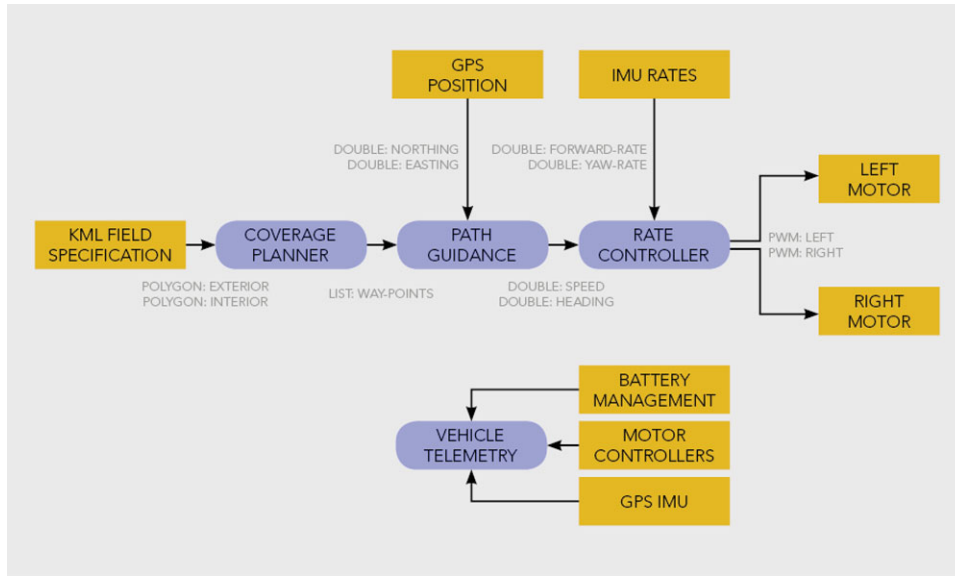We model the weeding mechanism with the following assumptions:

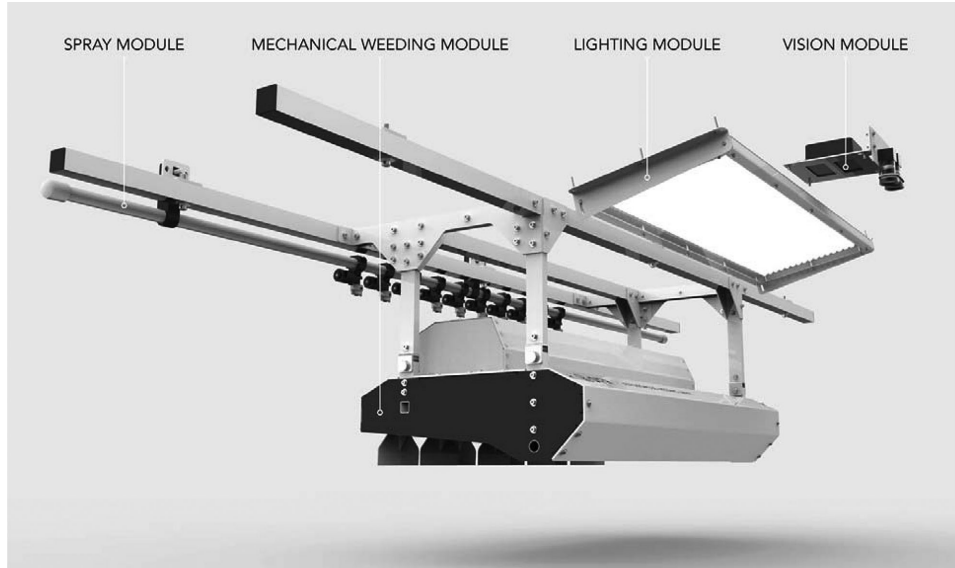**FIGURE 11** Simplified overview of the software for the navigation

FIGURE 12 Weeding implement system modules

- The weeding array has n identical weeding implements of width w.

- Each weed is treated by engaging one weeding implement for a fixed distance d.

- Weeds are uniformly distributed with a density λ weeds/m^2, so they arrive according to a Poisson process with an arrival rate of $\lambda \times w$.

- Power and traction limitations mean that only m out of n implements can be engaged at once, meaning some weeds may be missed.

This configuration is shown in Figure 14(a) and can be modeled as a M/D/c/c queuing theory problem. In this case, we can apply the Erlang B formula[72] to calculate probability of targeting a weed:

$$P_w(a, m) = 1 - \frac{a^m/m!}{\sum_m^{i=0} a^i/i!},\qquad(1)$$

where $a = \lambda wd$. Notice the probability of treating a weed P_w depends only on the parameters a and m. This formula allows us to trade off the maximum weed density, width, and soil engagement length when designing a mechanical weeding array. For convenience, Table II shows the values of λwd for $P_w(a, m) = 0.95$ for various values of m. For the AgBotII, the implement width is 1 m and the engagement length is 0.2 m, which requires $m \geq 2$, meaning the vehicle must be able to engage at least two weeding tools simultaneously. When the implement is extended to a width of 3 m, we require $m \geq 3$. Both of these are quite achievable given the small draft force of each weeding implement.

5.1.2 | 2DOF weeding mechanism analysis

The second configuration we examine is a 2DOF weeding tool. In this configuration, we have an implement of width w with a single weeding tool that can slide sideways and be lowered into the soil. This
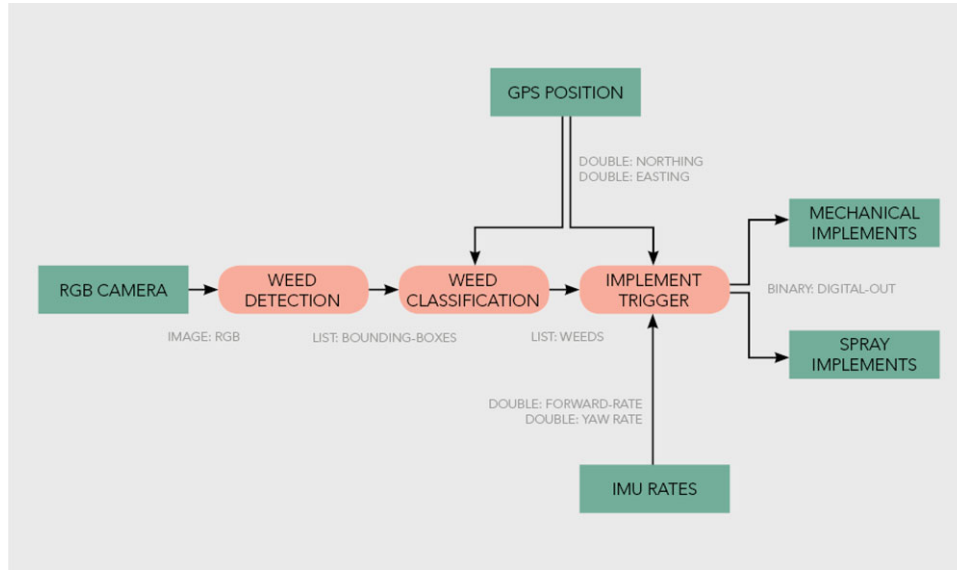
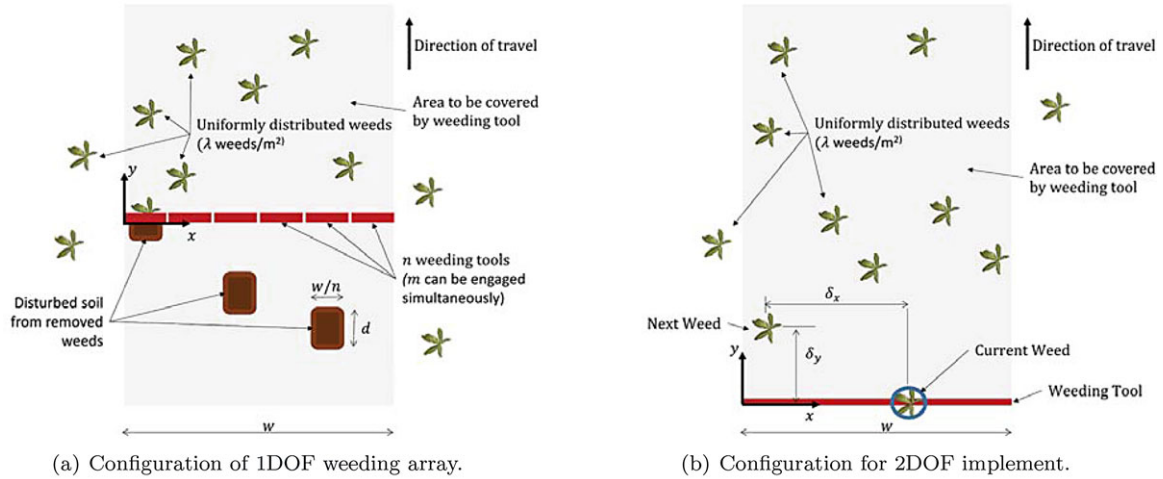**FIGURE 13** An overview of the software for the weeding system

(a) Configuration of 1DOF weeding array.

(b) Configuration for 2DOF implement.

FIGURE 14 The 1DOF configuration in (a) has n parallel weeding implements, of which m implements may engage the ground simultaneously, each for a distance of d. For the 2DOF configuration in (b), a single weeding tool can slide sideways to meet an approaching weed. After treating a weed, the tool must slide sideways a distance of δ_x before the next arrives in a δ_y

TABLE II Values a for $P_w = 0.95$ for various values of m

m	1	2	3	4	5	6
$a = \lambda w d$	0.053	0.38	0.90	1.52	2.22	3.00

configuration is shown in Figure 14(b). For simplicity, we ignore the tool engagement length and optimistically assume the weeding tool instantaneously removes each weed as long as the weeding tool can reach each weed in time. As the vehicle drives through the field at a constant velocity, the distance the vehicle drives between weeds will follow a Poisson process since we assume that weeds are uniformly distributed. Therefore, for an implement of width w and a weed density of λ, the interarrival distance of weeds in the direction of travel, δ_y, has a probability density function

$$f(\delta_y) = \lambda w e^{-\lambda w \delta_y}. \tag{2}$$

The location of weeds in the x axis forms a uniformly distributed random variable x with a probability density function

$$f(x) = \begin{cases} \frac{1}{w} & \text{for } 0 \leq x \leq w, \\ 0 & \text{otherwise.} \end{cases}$$

The (unsigned) distance the weeding tool must travel in order to get to the next weed is $\delta_x = |x_n - x_{n-1}|$, where x_n is the x offset of the nth weed. This offset δ_x varies between 0 and w with a one-sided triangle probability distribution function:

$$f(\delta_x) = \begin{cases} \frac{2}{w}\left(1 - \frac{\delta_x}{w}\right) & \text{for } 0 \leq \delta_x \leq w, \\ 0 & \text{otherwise.} \end{cases} \tag{3}$$

If we ignore the time required for acceleration, in order for the tool head to slide sideways to reach the next weed in time, we must satisfy

$$\frac{v_y}{v_x} \leq \frac{\delta_y}{\delta_x},$$

where v_y is the forward velocity of the vehicle and v_x is the maximum velocity of the sliding mechanism. The probability of reaching the next weed is therefore

$$P_w = P\left(\frac{v_y}{v_x} \leq \frac{\delta_y}{\delta_x}\right)$$

$$= P(v_y\delta_x - v_x\delta_y \leq 0).$$

The probability of treating a weed is therefore the sum of two scaled random variables $v_y\delta_x$ and $-v_x\delta_y$. For independent random variables, the density of their sum is the convolution of their densities. It follows from Eqs. (2) and (3) that the probability of treating a weed is

$$P_w = \frac{2(e^{-a} - 1 + a)}{a^2},$$

where $a = w^2 \lambda \frac{v_y}{v_x}$. We can see that the probability of treating a weed P_w only depends on the value a. For our target value of $P_w = 0.95$ and $\lambda = 1$ weed/m^2, we must satisfy $a \leq 0.16$. The implement is 1 m wide, which equates to $\frac{v_y}{v_x} \geq 6.25$, and for a typical forward vehicle velocity of 0.8 m s^{-1}, this equates to a slide mechanism that must be able to move at least 5.1 m s^{-1} without considering acceleration time and the time required to treat each weed. The high actuation speeds and accelerations required make this design complex to implement and impractical for larger slide widths w or higher weed densities λ. For those reasons, we chose not to pursue this design further.

5.2 | Weeding module design

A downward-facing camera is mounted on the front of the AgBotII looking directly down. The camera is mounted at a height such that its field of view is 1 m wide. The particular camera used was an IDS UI-1240SE 1.3MP global shutter camera. The camera is triggered at 5 Hz externally by a microcontroller, synchronized with a pulsed light module producing 50,000 lm for 2 ms. The light is placed at a slight angle to minimize specular reflections in the camera image, and it is pulsed to reduce energy consumption.

Once a weed is no longer in the field of view of the camera, its position relative to the robot needs to be estimated based on the robot's trajectory. To achieve this, the location of each weed is immediately transformed into the global frame using the GPS/INS and saved in a list. Each weed is then transformed back into the robot's frame on each new robot location measurement until the weed passes underneath an implement. A weed is considered to be under an implement if any part of its convex hull lies within the implement's target region. The INS is also used to compensate for physical delays in the weeding actuation.

The mechanical weeding implement is illustrated in Figure 15(a). It consists of an array of nine independent weeding tools, each of which is actuated via a spring-return pneumatic cylinder. An air compressor and accumulator tank onboard the AgBotII supplies compressed air to the weeding module actuators. The mechanical weeding module is

attached with four locking pins to the undercarriage of the AgBotII via a lightweight aluminum subframe.

The weeding tools have been designed to be removable and interchangeable. Tools can be specially designed for use on different weed varieties, soil densities, and soil types. For the prototype, a broad hoe style tool was used for weed removal, as shown in Figure 15(a).

The spray weeding module is comprised of ten solenoid-operated spray nozzles attached to a wet boom, which is supplied with water from the onboard 200 L spray tank via a 12 V 7.4 L min^{-1}. For field trials, the spray nozzles were adjusted to a thin stream so the accuracy and timing of the system could be clearly visualized from the marks on the ground and video data. Figure 15(b) shows the spray module targeting two weeds.

5.3 | Weed detection algorithms

Several methods to perform weed detection have been proposed, most of which make use of the normalized difference vegetation index (NDVI),[73] which is a combination of color (RGB) and near-infrared (NIR) information. RGB-NIR cameras for outdoors are typically expensive and of limited availability. A dual camera setup, with one RGB and one NIR camera, results in poor registration because of the variability in the ground plane and the weed height. Thus, we proceeded with a color-only based detection approach.

Inspired by Philipp and Rath,[56] we explored multiple color spaces to select the most suitable spaces for weed detection. It is well known that the RGB color space is extremely dependent upon illumination conditions, thus we investigated the use of color-opponent color spaces and cylindrical representations, which provide some inherent robustness to illumination. We considered the following four color spaces:

HSV is a cylindrical color space consisting of hue (H), saturation (S), and value or brightness (V).

YCbCr consists of luminance (Y), blue difference chroma (Cb), and red difference chroma (Cr).

Luv is a perceptually uniform color space where lightness is captured by the component L.

Lab is an opponent color space where a and b are the color-opponent dimensions.

We explored ways to develop robust features from these color spaces by removing the component that is most dependent upon intensity and also by combining the color spaces. The four color spaces that we explored all represent lightness (or brightness) using one component. This is in contrast to the RGB space, where lightness is present in all three components.

Combining the color spaces is explored as they provide complementary representations of the same information. To combine the color spaces, we concatenate the representation of two or more color spaces to form a combined color feature vector; for example, uvab is the vector for the combination of Luv and Lab. We show experimentally that this provides a consistently superior performance.

The color information of weeds, encoded using the color spaces (or combinations thereof), is modeled using a multivariate Gaussian,
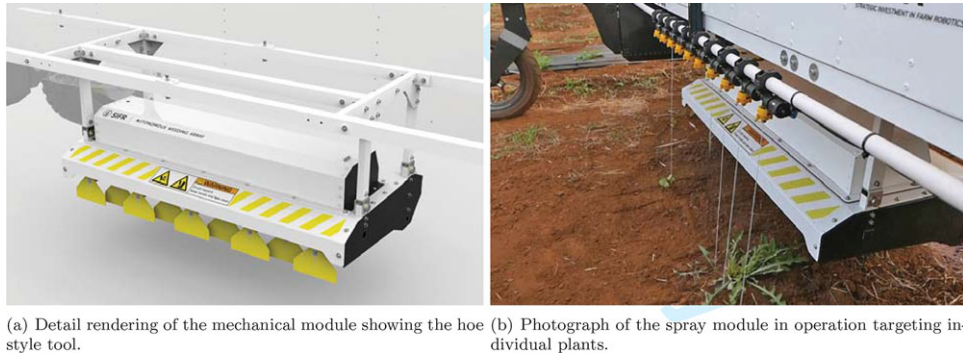
(a) Detail rendering of the mechanical module showing the hoe style tool. (b) Photograph of the spray module in operation targeting individual plants.

FIGURE 15 The mechanical and spray weeding modules form the plant-species–specific weed management system on the AgBotII
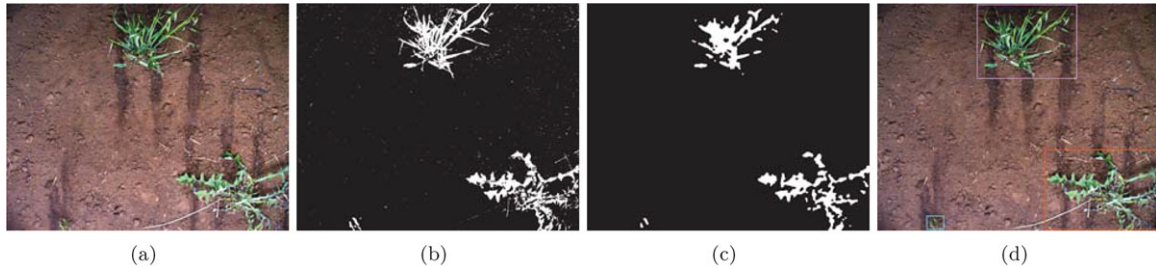

(a) (b) (c) (d)

FIGURE 16 From left to right: (a) the original image, (b) the result of per-pixel segmentation after thresholding, (c) the filtered image after erosions and dilations, and (d) the detection regions, indicated by the bounding boxes, where the different colors indicate the different species of weed: blue for Cotton, magenta for Wild Oats, and red for Sowthistle

$p(\mathbf{x} \mid \mu, \Sigma)$, where $\mathbf{x}$ is the feature vector, that is the color space representation, and the parameters (μ and Σ) are the model parameters learned on a training set of manually annotated images; Σ is assumed to be diagonal. A multivariate Gaussian is used because it can efficiently calculate the log-likelihood that a pixel $\mathbf{x}$ is a weed. This provides a per-pixel log-likelihood map, or segmentation map, similar to that in Figure 16(b).

To convert the segmentation map into weed regions, we first remove noise from the image and then search for connected regions. The per-pixel segmentation image will often be noisy, as can be seen in Figure 16(b), and we de-noise it by applying a set of erosions and dilations. In particular, we apply an erosion of size $S = 4$ pixels to remove small regions of noise, followed by a dilation of $S = 8$ pixels to join close regions, and finally an erosion of $S = 5$ pixels to shrink the artificially expanded regions. Contiguous regions are then found from this binary image by finding the contours.[74] Those regions that are close to one another, within 40 pixels or 4 mm, are merged to form a single weed. Finally, the bounding box of the contours is used for classification, as shown in Figure 16(d), and the convex hull of the contours is used to represent the weed for the purposes of triggering the weeding implements.

5.4 | Weed classification algorithms

To identify the species of weed, we consider two computationally efficient approaches, one based on the well-known local binary pattern features (LBP)[60] and the other on covariance features.[61]
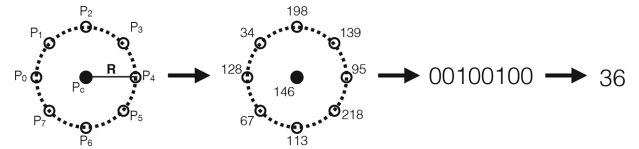

FIGURE 17 An overview of how local binary patterns are encoded. There are $P = 8$ sampling points taken from a circle of radius $R = 2$. A pixelwise comparison, to the central pixel, is performed to obtain a binary string, which can then be converted to an integer value

5.4.1 | Local binary pattern features

The LBP is computationally efficient and robust to illumination variations as it is computed by performing a set of pixel comparisons. The pixel of interest (central pixel) P_c is compared to the P surrounding pixels inside a radius of R resulting in a code given by

$$\text{LBP}_{P,R} = \sum_{p=0}^{P-1} h\left(P_c, P_p\right) 2^p, \tag{4}$$

where P_p is the value of the pth pixel, and

$$h(x, y) = \begin{cases} 1 & \text{if } y \geq x, \\ 0 & \text{if } y < x, \end{cases} \tag{5}$$

is a thresholding function. In this work, we use $R = 2$ and $P = 8$, as illustrated in Figure 17. To summarize a region, we collate the LBP responses over that region as a histogram,[62] which is a compact and efficient representation.

5.4.2 | Covariance features

Covariance features capture the gradient information from an area and then represent this compactly using a covariance matrix.[61,65] For each pixel, the following gradient information is extracted:

$$
\mathbf{y} = \left[r, g, b, |I_x|, |I_y|, |I_{xx}|, |I_{yy}|, \sqrt{I_x^2 + I_y^2}, \arctan \frac{|I_y|}{|I_x|} \right], \qquad (6)
$$

where $|I_x|$, $|I_y|$, $|I_{xx}|$, and $|I_{yy}|$ are the first- and second-order gradients of the grayscale image at the pixel locations (x, y); $\sqrt{I_x^2 + I_y^2}$ and $\arctan \frac{|I_y|}{|I_x|}$ correspond to the gradient magnitude and orientation, respectively; and r, g, and b correspond to the red, green, and blue values at the pixel location (x, y). Using this, each pixel is represented by a nine-dimensional feature vector. A region is then represented compactly using the covariance matrix ϕ,

$$
\phi = \frac{1}{N} \sum_{n=1}^{N} \left(\mathbf{y} - \mu_\mathbf{y} \right) \left(\mathbf{y} - \mu_\mathbf{y} \right)^T. \qquad (7)
$$

This covariance matrix now represents the information from the vegetation region, and it can be used to identify the species of plant.

5.4.3 | Species classification

Using both the LBP or covariance features, we classify the species of plant in the following manner. From a training set of images, we extract the features for the T_s instances of the sth species of plant. The feature representing the detected region is then compared to the training samples of each species, and the top N responses (most similar) for each species are then averaged using

$$
C_s = \frac{1}{N} \sum_{n=1}^{N} C_{s,n}, \qquad (8)
$$

where $C_{s,n}$ is the nth best score of the sth species, and for our work we use $N = 5$. We then choose the most likely species as the one with the highest similarity,

$$
T_s = \operatorname*{argmax}_{s=1,\dots,S} C_s. \qquad (9)
$$

The measure of similarity that we use for these two features is the squared cosine and symmetric Stein divergence for LBP and covariance features, respectively. We use the symmetric Stein divergence for covariance features as this exploits the fact that covariance matrices lie on a Riemannian manifold.[65] The symmetric Stein divergence is given by

$$
S(\mathbf{A}, \mathbf{B}) = \log \left[\det \left(\frac{\mathbf{A} + \mathbf{B}}{2} \right) \right] - \frac{1}{2} \log \left[\det (\mathbf{AB}) \right], \qquad (10)
$$

where $\mathbf{A}$ and $\mathbf{B}$ are the two covariance matrices to compare, and $\log$ in this case refers to a matrix logarithm.

6 | RESULTS

The plant-species–specific management was experimentally verified in three stages. The first step was to test the overall concept and system design in simulation. The second stage was to demonstrate the weed detection using an image database and then with the deployment of the system to a real agricultural task. The final stage was to determine the effectiveness of the weed-species classification using an image database and then using a field trial.

6.1 | Simulation

The AgBotII is simulated using a model for the two drive units based on experimental data from a dynamometer and a simplified model for the physical characteristics of the chassis and each of the four wheels. The weeding camera is simulated to randomly perceive weeds at a rate according to the distribution in Section 5.1. The simulated weeds also vary in location, shape, size, and species. The weeding implements are modeled as rectangular areas that illuminate when activated by the system. Figure 18(a) shows the two implement rows, the blue row for the spray and the yellow for the mechanical, with an incoming weed shown by the yellow polygon. Figure 18(b) is a broader picture of the simulation showing the entire system described in Sections 4.3 and 5. The comprehensive simulation shown in the figures was vital to the rapid deployment of the AgBotII into the field once the hardware was completed.

(a) Simulated weed camera and weed implements.

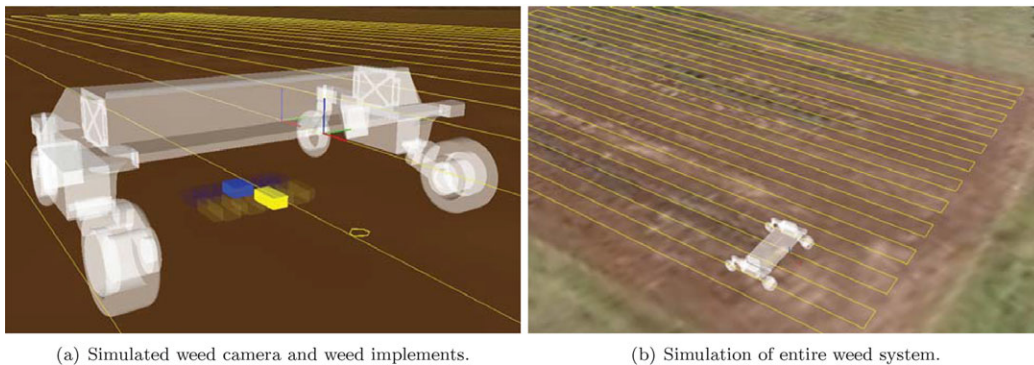(b) Simulation of entire weed system.

FIGURE 18 The system was tested in simulation prior to field testing. The image on the left shows the simulation of the weed detection and destruction, while the right image shows the simulation of the entire field used for the trials

TABLE III Results of the vegetation detection study in terms of the F_1 score

Luminosity	Colour feature	Eval.	Test
Yes	RGB	0.151	0.193
	YCbCr	0.598	0.653
	HSV	0.729	0.741
	Luv	0.782	0.820
	Lab	**0.888**	**0.868**
No	CbCr	0.808	0.847
	HS	0.842	0.862
	uv	0.883	0.891
	ab	**0.923**	**0.906**
No	uvabHS	**0.924**	**0.915**

6.2 | Weed detection

6.2.1 | Weed detection results on image dataset

To train, evaluate, and test the weed detection system, we collected a set of plant images. The plant images were collected using two cameras, the first being a Canon 7D, which is a high-quality digital single-lens reflex (SLR) camera, and the second being a high-end mobile phone (Sony XPeria Z3 Compact).* Twenty images were captured with each device, including images of a fallow field farm in Gatton, Queensland and garden beds in Brisbane, Queensland. The images were taken to include a variety of plants and illumination conditions including shadowing (see Fig. 19). The ground truth annotation denotes the location of each pixel of vegetation within the image, and it is used to train and evaluate the developed algorithms; the images were annotated by hand using a photoprocessing toolkit.

In total, 40 images were acquired and divided into three sets for training (14 images), evaluation (14 images), and testing (12 images). The training set was used to learn the parameters of the model. The evaluation set was used to evaluate the performance of the model using the F_1 score for the resultant precision-recall curve using the point at which the precision (P) is equal to the recall (R),

$$F_1 = 2 \times \frac{P \times R}{P + R}. \tag{11}$$

A threshold τ was then chosen at this point (from the evaluation set) and applied to the test set of images.

The results in Table III highlight the importance of removing the luminosity component from each color space. This leads to consistently improved performance and is a potential explanation as to why the RGB color space, which has no separate luminosity component, has significantly lower performance than any other color space. Experiments were also conducted to use multiple color spaces as a feature for each pixel.

We found that the best performing combination was the color components from Luv, Lab, and HSV, uvabHS, at 0.924. The uvabHS color space has slightly improved performance over using just the (L)ab color

space on the evaluation set, as well as better performance on the test set. We are able to achieve state-of-the-art results using only a single camera without infrared information, in contrast to NDVI. Given this result, we use the uvabHS color space based system as our method for detecting weeds in later field trials.

6.2.2 | Weed detection results from field trial

The AgBotII and weed management system were used to maintain a fallow field to be free of weeds. The AgBotII traversed the field twice per week for six weeks, removing the detected weeds using the mechanical implement. A scale map of the field used for the trial is shown in Figure 20(a). The field was approximately 1000 m^2; one-third of the field was selected to remain untouched as a control for the experiment, while the remaining two-thirds had the weeds removed by the AgBotII. The rows to be used as controls were selected at random, and their distribution is shown in Figure 20. The field was initially ploughed using a large tractor and then left alone to allow the weeds to emerge naturally. The field has a very large seed bank ensuring the growth of a large number of weeds.

The coverage of weeds in the control and treated rows was recorded on each iteration over 42 days. The amount of soil tilled by the mechanical implements was also recorded on each iteration. There was a significant rain event early in the experiment that caused a very large number of weeds to germinate at the same time; between day 17 and 24 the weed density in the field increased from 0.12 to 37 weeds per m^2.

Figure 21 shows the growth of the weeds and the treatment of the weeds in the field over time. Figure 21(a) displays the percentage of weed coverage in the treated and control sections of the field. It is clear that after the rain event, the amount of weed coverage in the control grew rapidly to 37%. However, the coverage in the treated area grew slowly, peaking at 4.5%, then receding to 1.5%, remaining nonzero as new weeds are continuously germinating in the field. This result simultaneously demonstrates the abilities of the weed detection technique and the efficacy of the mechanical implement.

Figure 21(b) shows the percentage of the treated sections that were tilled by the mechanical implement. The figure shows that a significant percentage of area was not tilled on each traversal of the AgBotII. Minimizing the amount of area tilled has potential benefits in soil fertility due to improved moisture and organic matter retention.

The results of the experiment can be visualized by looking directly at an image of the field. Figure 22 shows an ultrahigh-resolution mosaic created by stitching the images collected by the AgBotII. The breakout images on the right show increasingly zoomed images of the same section of field.

6.3 | Weed classification

6.3.1 | Weed classification results from glasshouse experiments

A set of trials was conducted in a controlled glasshouse with a variety of broad-leaf and grass weeds recognized as being of high importance for eradication by Queensland broadacre farmers. These included

---

* The DSLR images had an image resolution of 2592 × 1728, and the mobile phone images had an image resolution of 3840 × 2160.

(a) Example digital SLR image.   (b) Example mobile phone image.

FIGURE 19   Example images used to train and evaluate the weed detection algorithm

(a) The yellow rows indicate the treated sections of the field while the green sections were left as controls.   (b) Photo of the field at the conclusion of the trial. The treated and control sections of the field are easily distinguished.

FIGURE 20   The field used for the trial

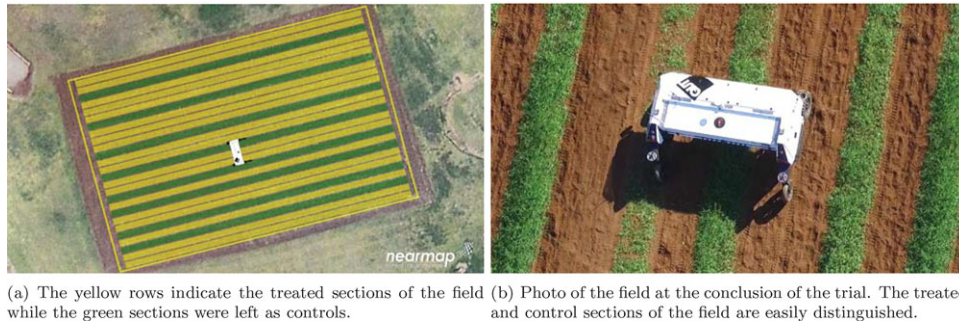(a) The percentage of the field covered in weeds.   (b) The percentage of the field mechanically treated.
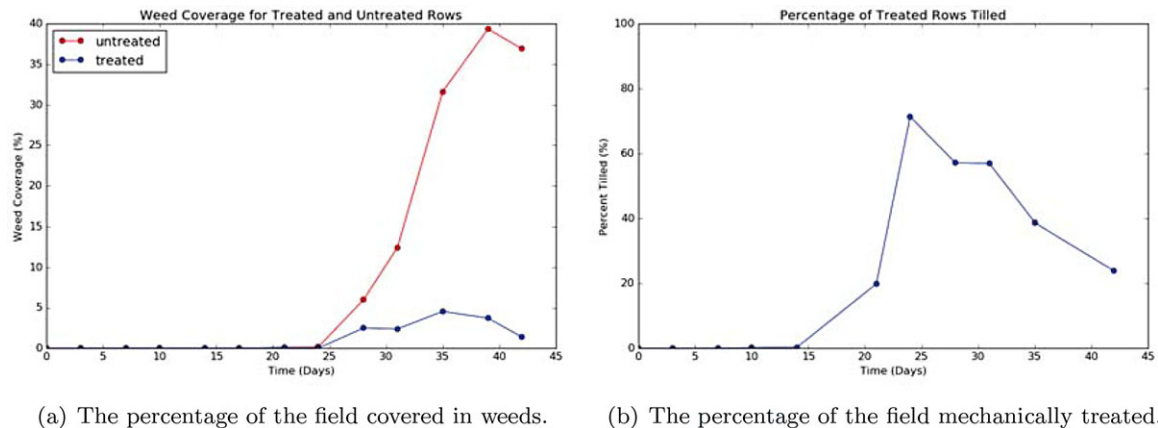
FIGURE 21   Weed growth and subsequent weed treatment over time during the trial

Feathertop Rhodes Grass, Barnyard Grass, Wild Oats, Sowthistle, Fleabane, and Volunteer Cotton.

From the six species of plants grown, five species successfully grew in the environment: Feathertop Rhodes Grass (GR), Barnyard Grass (GR), Wild Oats (GR), Sowthistle (BL), and Cotton (BL); Fleabane did not germinate for these experiments. Imagery was taken periodically of these plants as they grew, and they were used as a dataset for evaluation of the two potential weed classification techniques.

It can be seen in Figure 23 that the covariance features (Cov.) consistently outperform the LBP features. From this result, the classification method deployed on the AgBotII for field trials used the Cov. features. Detailed results of the performance of the Cov. features can be seen as a confusion matrix in Table IV. This table also groups the results in terms of "plant group"; grass (GR) or broad-leaf (BL). It can be seen that the group-based identification (identifying a grass as being one of the

grasses) was 96.0% for grass and 95.9% for broad-leaf. This shows the potential for this algorithm to be used to classify plants into two plant groups. Furthermore, the identification rate for Volunteer Cotton was 98.8%, an impressive result, which shows the potential of the system to be used to identify crops that are visually distinctive, such as Cotton.

6.3.2 | Weed classification results from field trial

To evaluate the effectiveness of the weed classification, a field trial was conducted with a small selection of high importance weeds. The six weed types previously used in the glasshouse were planted in a small field that was otherwise maintained to be free of other weeds. Unfortunately, only three weed species germinated: Wild Oats, Sowthistle, and Volunteer Cotton. Images of the weeds in the field were captured approximately every 2 weeks to further test and refine the
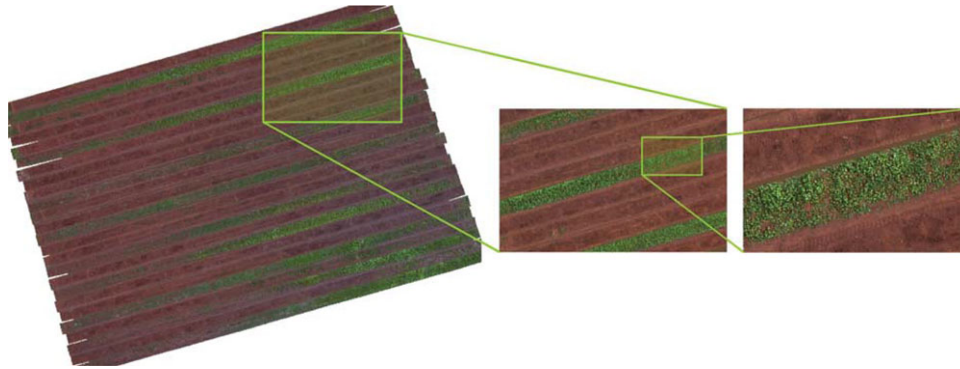
FIGURE 22 The field at the end of the trial clearly showing the difference in weed density between the treated and untreated sections

TABLE IV Glasshouse trial results for covariance features as a confusion matrix. Rows correspond to particular weed species. Columns show the percentage of instances that weed images are declared as belonging to a particular species. The results in blue correspond to Broad-leaf weeds, while those in green correspond to Grass weeds

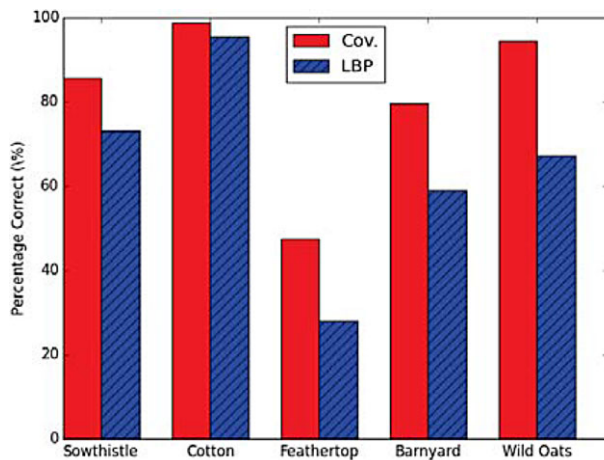|	Sowthistle (BL)	Cotton (BL)	Feathertop (GR)	Barnyard (GR)	Wild Oats (GR)
Sowthistle (BL)	**85.6%**	6.2%	1.1%	2.3%	4.8%
Cotton (BL)	1.1%	**98.8%**	0.0%	0.1%	0.0%
Feathertop (GR)	1.6%	0.0%	**47.5%**	47.5%	3.3%
Barnyard (GR)	3.5%	0.0%	8.0%	**79.5%**	9.0%
Wild Oats (GR)	0.6%	0.0%	2.5%	2.5%	**94.3%**

FIGURE 23 The accuracy of the two methods, Cov. and LBP, on the data collected from the Glasshouse

classification algorithms. The heterogeneous weeding array was configured so that the Volunteer Cotton was treated with the spray implement, while the Sowthisle and Wild Oats were selected for destruction using the mechanical implement.

Figure 24 provides an example image taken from the trial where all three weed species have been correctly classified. The classification results, shown in Table V, highlight the effectiveness of the proposed system. With the three weed species grown in the field, the average classification success rate was 92.3%. This means 7.7% of the time weed species were misclassified and targeted incorrectly. That is, Cotton was incorrectly destroyed with the mechanical implement, or Sowthistle and Barnyard Grass were incorrectly treated with spray. However, 100% of the plants were detected and treated with a
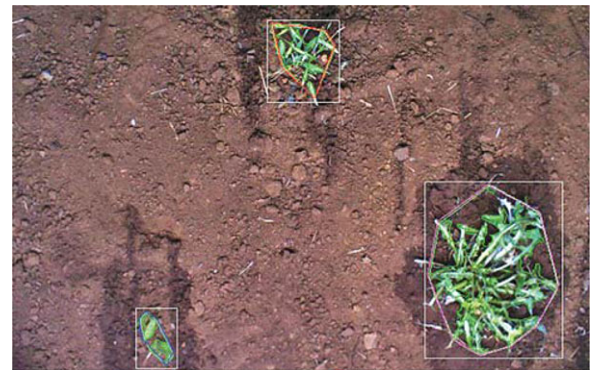

FIGURE 24 An example image of the weed detection and classification. Cotton is highlighted by the blue polygon region, Wild oats is highlighted in red, and Sowthistle surrounded by the magenta polygon

TABLE V Field trial results for classification as a confusion matrix. Rows correspond to particular plant species. Columns show the percentage of instances that plant images are declared as belonging to a particular species

	Cotton	Wild Oats	Sowthistle
Cotton	**97.8%**	0.5%	1.7%
Wild Oats	0.8%	**97.3%**	1.9%
Sowthistle	17.2%	0.8%	**82.0%**

weeding implement. Figure 25(a) shows an example where Cotton is targeted for spraying while the Wild Oats is being removed using the mechanical implement [Fig. 25(b)].

Figures 25(b) and 26 illustrate the effectiveness of the mechanical implement in removing weeds. Figure 25(b) shows a closeup
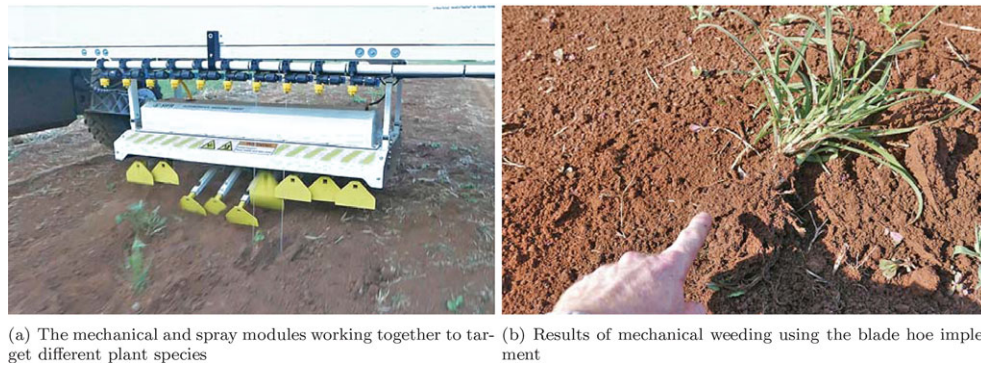
(a) The mechanical and spray modules working together to target different plant species

(b) Results of mechanical weeding using the blade hoe implement

FIGURE 25 Multi-mode weed management in action on the AgBotII

(a) Before and after of destruction of Sowthistle

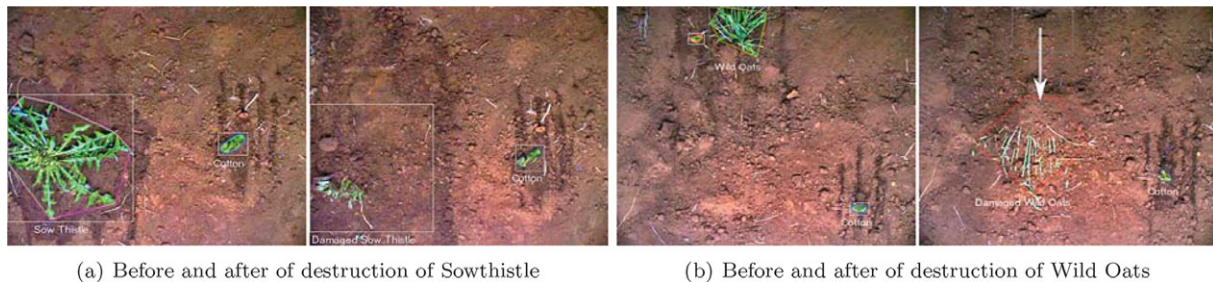(b) Before and after of destruction of Wild Oats

FIGURE 26 Images of weeds successfully targeted with the mechanical implement

photograph of an uprooted Wild Oats plant, while Figure 26 shows before and after photos of the treated weeds. A video summarizing the results of the plant-species–specific treatment of weeds can be found at the following location: https://goo.gl/mJxqjM.

7 | CONCLUSION

This paper describes the design, development, and testing of a robot for plant-species–specific weed management. The design of a robotic system to best satisfy the required objectives is a complex task. We took a proven approach and described how we analyzed insights from farmers to form specifications for the design. Furthermore, the design of AgBotII has been conducted such that with suitable modifications, the platform could be commercialized for different applications in agriculture. As such, aspects of the design have contemplated manufacturing, working spaces, assembly, and potentially shipping.

Field trials have demonstrated the potential of this autonomous system for individualized treatment of weeds. The in-field experiments for vision-based weed detection and classification highlight the fact that the system is able to detect and classify accurately, online, a range of weed species. In particular, a trial of the AgBotII in a fallow field over six weeks maintained the weed coverage in treated sections to be 1.5%, compared to 37% in the control areas. This demonstrates the effectiveness of the weed detection system and the selective mechanical implement.

Another trial showed that the weed classification system was able to classify broad-leaf and grass plants with an accuracy of 96% and classify individual weed species with an accuracy of 92.3%. The weed classification system was used online with the heterogeneous weeding array to selectively spray a particular weed species and mechanically remove another weeds species based on visual information.

Robotic technology is transforming current practices in many industry sectors. Following this trend in research and development activities worldwide, we envisage that this technology will also soon have a significant impact in agricultural practices. The process followed in this paper for the specification, design, and in-field testing of a robot for weed management has proven to be effective. We expect that this process can be of guidance in future developments and be adapted to other applications, and that further innovative implements can be mounted on the robot.

Future work will concentrate on enhancing the robustness of the vision system to cope with changes in lighting conditions in daytime operation and the efficacy of various mechanical methods for different weed species in different soil types. The latter shall determine optimal implements for classes of species and specific paddocks.

REFERENCES

1. UN How to feed the world in 2050. Technical report, Food and Agriculture Organisation, United Nations. 2009.

2. Alakukku L, Weisskopf P, Chamen W, et al. Prevention strategies for field traffic-induced subsoil compaction: A review: Part 1. Machine/soil interactions. *Soil Tillage Res*. 2003;73:145–160.

3. Raper R. Agricultural traffic impacts on soil. *J Terramechanics*. 2005;42(3–4):259–280.

4. Llewellyn R, D'Emden FH. Adoption of no-till cropping practices in Australian grain growing regions. Technical report, Grains Research and Development Corporation, Australian Government. 2010.

5. Sinden J, Jones R, Hester S, et al. The economic impact of weeds in Australia. Technical report, CRC for Australian Weed Management. 2004.

6. Charles G, Leven T. Integrated weed management for Australian cotton. In *Cotton Pest Management Guide*, Australia: CRC; 2011:88–119.

7. Daniel R, Simpfendorfer S, Serafin L, et al. Choosing Rotation Crops: Fact Sheet. Technical report, Grains Research and Development Corporation, Australian Government. 2011.

8. Newman P, Zaicou-kunesch C. Economic activity attributable to crop protection products. Technical report, Department of Agriculture and Food, Government of Western Australia. 2013.

9. Day W. Engineering advances for input reduction and systems management to meet the challenges of global food and farming futures. *J Agricult Sci*. 2011;149:55–61.

10. Kassler M. Agricultural automation in the new millennium. *Comput Electron Agricult*. 2001;30:237–240.

11. IAgrE Agriculture engineering: A key discipline enabling agriculture to deliver global food security. Technical report, Institution of Agricultural Engineers, UK. 2013.

12. Bawden O, Ball D, Kulk J, et al. A lightweight, modular robotic vehicle for the sustainable intensification of agriculture. In *Proceedings of Australasian Conference on Robotics and Automation*. 2014.

13. Bekker MG. *Theory of Land Locomotion: The Mechanics of Vehicle Mobility*. University of Michigan Press; 1956.

14. Bekker MG. *Off-the-road Locomotion: Research and Development in Terramechanics*. University of Michigan Press; 1960.

15. Wong JY. *Terramechanics and Off-road Vehicle Engineering: Terrain Behaviour, Off-road Vehicle Performance and Design*. Butterworth-Heinemann; 2009.

16. Apostolopoulos D. Analytic configuration of wheeled robotic locomotion. Technical report, Carnegie Mellon University, Pittsburgh, PA, 2001.

17. Madsen TE, Jakobsen HL. Mobile robot for weeding. Master's thesis, Technical University of Denmark. 2001.

18. Åstrand B, Baerveldt A-J. An agricultural mobile robot with vision-based perception for mechanical weed control. *Auton Robots*. 2002;13(1):21–35.

19. Jensen K, Nielsen S, Joergensen R, et al. A low cost, modular robotics tool carrier for precision agriculture research. In *Proceedings of International Conference on Precision Agriculture*. 2012.

20. Bakker T, Asselt K, Bontsema J, et al. Systematic design of an autonomous platform for robotic weeding. *J Terramechanics*. 2010;47(2):63–73.

21. Ruckelshausen A, Biber P, Dorna M, et al. Bonirob—An autonomous field robot platform for individual plant phenotyping. *Precision Agricult*. 2009;9(841).

22. Jorgensen R, Sorensen C, Maagaard J, et al. Hortibot: A system design of a robotic tool carrier for high-tech plant nursing. *Agricult Eng Int: CIGR J*. 2007;9.

23. Ruckelshausen A, Klose R, Linz A, et al. Autonomous robots for weed control. *J Plant Diseases Protection*. 2006;173–180.

24. Tressos K, Andreou I, Gemtos T, et al. Zeus—Supportive autonomous vehicle for agriculture. 2011. Online. University of Thessaly, http://www.savage.gr.

25. Underwood JP, Calleija M, Taylor Z, et al. Real-time target detection and steerable spray for vegetable crops. In *Proceedings of IEEE International Conference of Robotics and Automation Workshop on Robotics in Agriculture*. 2015.

26. Schulz K, Anderson T. Spirit—Tractor platform. 2014. Online. Autonomous Tractor Corporation, http://www.autonomoustractor.com/.

27. Brixius W, Zoz F. Tires and tracks in agriculture. SAE Technical Paper, SAE International. 1976.

28. Molin J, Leviticus L. Performance and use of tracks in agriculture—A review. SAE Technical Paper, SAE International. 1995.

29. Green O, Schmidt T, Pietrzkowski RP, et al. Commercial autonomous agricultural platform—kongskilde robotti. In *Proceedings of the International Conference on Robotics, Associated High-technologies and Equipment for Agriculture and Forestry*. 2014.

30. Tillett N, Hague T, Grundy A, et al. Mechanical within-row weed control for transplanted crops using computer vision. *Biosyst Eng*. 2008;99(2):171–178.

31. Stektee Steketee IC. 2017. Online. http://www.steketee.com/product/Steketee-IC.

32. Dedousis A. An investigation into the design of precision weeding mechanisms for inter or intra-row weed control. Ph.D. thesis, Cranfield University, UK. 2007.

33. Griepentrog HW, Gulholm-Hansen T, Nielsen J. First field results from intra-row rotor weeding. In *Proceedings of EWRS Workshop on Physical and Cultural Weed Control*. 2007.

34. Griepentrog HW, Nørremark M, Nielsen J. Autonomous intra-row rotor weeding based on GPS. In *Proceedings of World Congress on Agricultural Engineering for a Better World*. 2006.

35. Home M. An investigation into the design of cultivation systems for inter-and intra-row weed control. Ph.D. thesis, Cranfield University, UK. 2003.

36. Van Der Weide R, Bleeker P, Achten V, et al. Innovation in mechanical weed control in crop rows. *Weed Res*. 2008;48(3):215–224.

37. Poulsen F. Engineering Robovator—Mechanical. 2017. Online. http://www.visionweeding.com/robovator-mechanical/.

38. Schans D, Bleeker P. Practical weed control in arable farming and outdoor vegetable cultivation without chemicals. CAB International. 2006.

39. Blasco J, Aleixos N, Roger J, et al. Robotic weed control using machine vision. *Biosyst Eng*. 2002;83(2):149–157.

40. Langsenkamp F, Sellmann F, Kohlbrecher M, et al. Tube stamp for mechanical intra-row individual plant weed control. In *Proceedings of World Congress of CIGR*. 2014.

41. Sellmann F, Bangert W, Grzonka S, et al. RemoteFarming. 1: Human-machine interaction for a field-robot-based weed control application in organic farming. In *Proceedings of International Conference on Machine Control and Guidance*. 2014.

42. University of Sydney. Agricultural Robotics at the Australian Centre for Field Robotics. 2017. Online. http://sydney.edu.au/acfr/agriculture.

43. ecoRobotix. Precise herbicide application with autonomous robot. 2017. Online. http://www.ecorobotix.com/.

44. Van Evert FK, Samsom J, Polder G, et al. A robot to detect and control broad-leaved dock (Rumex obtusifolius L.) in grassland. *J Field Robotics*. 2011;28(2):264–277.

45. Finze J, Bohm H. Effect of direct control measures and grazing management on the density of dock species (rumex spp.) in organically managed grassland. *J Plant Disease Protection*. 2004;19:527–535.

46. Jeon HY, Tian LF. Direct application end effector for a precise weed control robot. *Biosyst Eng*. 2009;104(4):458–464.

47. Shiraishi M, Sumiya H. Plant identification from leaves using quasi-sensor fusion. *J Manufact Sci Eng*. 1996;118(3):382–387.

48. Townshend JR, Justice C. Analysis of the dynamics of African vegetation using the normalized difference vegetation index. *Int J Remote Sens*. 1986;7(11):1435–1445.

49. Lin C. A support vector machine embedded weed identification system. Ph.D. thesis, University of Illinois at Urbana-Champaign, Urbana, IL. 2009.

50. Okamoto H, Murata T, Kataoka T, et al. Plant classification for weed detection using hyperspectral imaging with wavelet analysis. *Weed Biol Manage.* 2007;7(1):31–37.

51. Piron A, Leemans V, Lebeau F, et al. Improving in-row weed detection in multispectral stereoscopic images. *Comput Electron Agricult.* 2009;69(1):73–79.

52. Meyer GE, Neto JC. Verification of color vegetation indices for automated crop imaging applications. *Comput Electron Agricult.* 2008;63(2):282–293.

53. Carlson TN, Ripley DA. On the relation between ndvi, fractional vegetation cover, and leaf area index. *Remote Sens Environ.* 1997;62(3):241–252.

54. Suh H, Hofstee J, van Henten E. Shadow-resistant segmentation based on illumination invariant image transformation. In *Proceedings of International Conference of Agricultural Engineering.* 2014.

55. Ruiz-Ruiz G, Gómez-Gil J, Navas-Gracia L. Testing different color spaces based on hue for the environmentally adaptive segmentation algorithm. *Comput Electron Agricult.* 2009;68(1):88–96.

56. Philipp I, Rath T. Improving plant discrimination in image processing by use of different colour space transformations. *Comput Electron Agricult.* 2002;35(1):1–15.

57. De Smedt F, Billiauws I, Goedemé T. Neural networks and low-cost optical filters for plant segmentation. *Int J Comput Inform Syst Indust Manage Appl.* 2011;3:804–811.

58. Guyer DE, Miles G, Schreiber M, et al. Machine vision and image processing for plant identification. *Trans Am Soc Agricult Biolog Eng.* 1986;29(6):1500–1507.

59. De Rainville F-M, Durand A, Fortin F-A, et al. Bayesian classification and unsupervised learning for isolating weeds in row crops. *Pattern Anal Appl.* 2014;17(2):401–414.

60. Ojala T, Pietikainen M, Maenpaa T. Multiresolution gray-scale and rotation invariant texture classification with local binary patterns. *IEEE Trans Pattern Anal Machine Intell.* 2002;24(7):971–987.

61. Tuzel O, Porikli F, Meer P. Region covariance: A fast descriptor for detection and classification. In *Proceedings of European Conference on Computer Vision.* Springer; 2006:589–600.

62. Ahonen T, Hadid A, Pietikainen M. Face description with local binary patterns: Application to face recognition. *IEEE Trans Pattern Anal Machine Intell.* 2006;28(12):2037–2041.

63. McCool C, Sa I, Dayoub F, et al. Visual detection of occluded crop: For automated harvesting. In *Proceedings of IEEE International Conference on Robotics and Automation.* 2016.

64. Faraki M, Harandi MT, Porikli F. Approximate infinite-dimensional region covariance descriptors for image classification. In *Proceedings of IEEE International Conference on Acoustics, Speech and Signal Processing.* IEEE; 2015:1364–1368.

65. Sanin A, Sanderson C, Harandi MT, et al. Spatio-temporal covariance descriptors for action and gesture recognition. In *Proceedings of IEEE Workshop on Applications of Computer Vision.* 2013;103–110.

66. Gulliksen J, Göransson B, Boivie I, et al. Key principles for user-centred systems design. *Behav Inf Technol.* 2003;22(6):397–409.

67. Redhead F, Snow S, Vyas D, et al. Bringing the farmer perspective to agricultural robots. In *Proceedings of Conference on Human Factors in Computing Systems.* 2015;1067–1072.

68. Bawden OJ. Design of a lightweight, modular robotic vehicle for the sustainable intensification of broadacre agriculture. Master's thesis, Queensland University of Technology, Australia. 2015.

69. NTC (2015). Australian Light Vehicle Standards Rules 2015. Technical report, National Transport Commission, Australia. 2015.

70. Tritium. Tritium—iq battery management system. 2017. Online. Tritium Pty Ltd, http://tritium.com.au/.

71. Ball D, Ross P, English A, et al. Robotics for sustainable broadacre agriculture. In *Proceedings of Field and Service Robotics.* Springer; 2013:439–453.

72. Zeng G. Two common properties of the erlang-b function, erlang-c function, and engset blocking function. *Math Comput Modell.* 2003;37(12):1287–1296.

73. Kiani S. Discriminating the corn plants from the weeds by using artificial neural networks. *Int J Natural Eng Sci.* 2012;6(3):55–58.

74. Suzuki S, Abe K. Topological structural analysis of digitized binary images by border following. *Comput Vision, Graphics, Image Proc.* 1985;30(1):32–46.